Development 139, 4492 (2012) doi:10.1242/dev.090597


# Ptf1a control of Dll1 reveals an alternative to the lateral inhibition mechanism

**Jonas Ahnfelt-Rønne, Mette C. Jørgensen, Rasmus Klinck, Jan N. Jensen, Ernst-Martin Füchtbauer, Tye Deering, Raymond J. MacDonald, Chris V. E. Wright, Ole D. Madsen and Palle Serup**

There was an error published in *Development* **139**, 33-45.

On p. 36, Fig. 1 was incorrectly cited several times in place of Fig. 2. The correct paragraph appears below.

The authors apologise to readers for this mistake.

To determine if endodermal Notch activation and *Hes1* expression depends on Dll1 activity, we analyzed NICD expression in wild-type and $Dll1^{lacZ/lacZ}$ embryos and EGFP expression in crosses of $Tg(Hes1\text{-}EGFP)^{1Hri}$ and $Dll1^{lacZ/+}$ mice. NICD expression was reduced in E10.5 $Dll1^{lacZ/lacZ}$ embryos compared with controls (Fig. 2A,B), but appeared to recover, approaching wild-type levels at E11.5 (Fig. 2C,D). Hes1-EGFP expression was normal in E8.25 $Dll1^{lacZ/lacZ}$ embryos (Fig. 2E,I) but had partly disappeared from the dorsal pancreas endoderm at E9.5 (Fig. 2F,J) and was almost lost at E10.5 (Fig. 2G,K). Remarkably, and coinciding with the reappearance of NICD, Hes1-EGFP expression was restored in E11.5 $Dll1^{lacZ/lacZ}$ embryos (Fig. 2H,L).

Development 139, 33-45 (2012) doi:10.1242/dev.071761


# Ptf1a-mediated control of Dll1 reveals an alternative to the lateral inhibition mechanism

**Jonas Ahnfelt-Rønne[1,*], Mette C. Jørgensen[1,*], Rasmus Klinck[1], Jan N. Jensen[1], Ernst-Martin Füchtbauer[2], Tye Deering[3], Raymond J. MacDonald[3], Chris V. E. Wright[4], Ole D. Madsen[1] and Palle Serup[1,‡]**

## SUMMARY

Neurog3-induced *Dll1* expression in pancreatic endocrine progenitors ostensibly activates *Hes1* expression via Notch and thereby represses *Neurog3* and endocrine differentiation in neighboring cells by lateral inhibition. Here we show in mouse that *Dll1* and *Hes1* expression deviate during regionalization of early endoderm, and later during early pancreas morphogenesis. At that time, Ptf1a activates *Dll1* in multipotent pancreatic progenitor cells (MPCs), and *Hes1* expression becomes *Dll1* dependent over a brief time window. Moreover, *Dll1*, *Hes1* and *Dll1*/*Hes1* mutant phenotypes diverge during organ regionalization, become congruent at early bud stages, and then diverge again at late bud stages. Persistent pancreatic hypoplasia in *Dll1* mutants after eliminating *Neurog3* expression and endocrine development, together with reduced proliferation of MPCs in both *Dll1* and *Hes1* mutants, reveals that the hypoplasia is caused by a growth defect rather than by progenitor depletion. Unexpectedly, we find that *Hes1* is required to sustain Ptf1a expression, and in turn *Dll1* expression in early MPCs. Our results show that Ptf1a-induced Dll1 expression stimulates MPC proliferation and pancreatic growth by maintaining *Hes1* expression and Ptf1a protein levels.

**KEY WORDS: Dll1, Hes1, Neurog3, Notch, Pancreas, Ptf1a, Mouse**

## INTRODUCTION

Onset of Pdx1 expression in mouse posterior foregut endoderm around E8.0 marks the initiation of pancreas development. The first Neurog3$^+$ endocrine precursors (Gu et al., 2002) are found slightly later, between embryonic day (E) 8.5 and E8.75 (Jorgensen et al., 2007). *Neurog3* is required and sufficient for induction of pancreatic endocrine development (Apelqvist et al., 1999; Gradwohl et al., 2000; Schwitzgebel et al., 2000). Early Neurog3$^+$ precursors are increased in embryos deficient for the Notch pathway genes *Dll1*, *Rbpj* and *Hes1* (Apelqvist et al., 1999; Jensen et al., 2000b), and pancreatic expression of the Notch1 intracellular domain (NICD) represses endocrine as well as exocrine differentiation (Esni et al., 2004; Hald et al., 2003; Murtaugh et al., 2003). These findings led to the suggestion that Notch-mediated lateral inhibition prevents excessive endocrine differentiation of progenitor cells, thereby allowing ensuing proliferation and morphogenesis of pancreatic progenitor cells (Apelqvist et al., 1999; Edlund, 2002; Jensen et al., 2000b; Skipper and Lewis, 2000).

The lateral inhibition model posits that onset of Neurog3 expression in multipotent pancreatic progenitor cells (MPCs) initiates endocrine differentiation and activates expression of the Notch receptor ligand Dll1. Dll1 subsequently activates Notch receptors in neighboring cells, turning on *Hes1* expression in these. Hes1 then inhibits *Neurog3* expression, preventing adjacent cells from adopting an endocrine fate. However, the lateral inhibition model is largely based on the similar phenotypes seen in the above-mentioned mutants and most of the model's mechanistic predictions have not been tested rigorously. Also, major gaps exist in our understanding of the timing and extent of ligand expression and how it affects the behavior and number of MPCs as well as their progression to the defined endocrine/duct progenitors in the central epithelium versus acinar/duct progenitors of the peripheral epithelium at later stages (Kopinke et al., 2011; Schaffer et al., 2010). Further, recent studies imply that Notch-mediated regulation of endocrine differentiation is more complex than the model suggests. For example, while endocrine cells are formed continuously from E9.5 until birth, with a major burst in β-cell generation between E13.5 and E16.5 in the mouse, Notch ligand-receptor interactions are thought to change as development proceeds, either by temporally controlled activation of different ligands or through different affinities for different Notch ligand-receptor pairs.

Dll1 is the first ligand to be expressed in the pancreatic epithelium, together with the receptors Notch1 and Notch2, and Dll1 appears to be the only ligand expressed between E9.5 and E11.5 (Apelqvist et al., 1999; Lammert et al., 2000). However, Jag1 expression begins around E12 and becomes the most abundant ligand in the pancreas epithelium at mid-gestation (Golson et al., 2009; Lammert et al., 2000). Also, while a Ptf1a$^{Cre}$-mediated, pancreas-specific knock-out of *Rbpj* (Fujikura et al., 2006) shows increased numbers of Neurog3$^+$ cells at E10.5, these animals showed decreased Neurog3$^+$ cells at E11.5, and the pancreas was not hypoplastic as seen in *Hes1* mutants (Jensen et al., 2000b). It was suggested that progenitors competent to initiate endocrine development become depleted very early and quite specifically if Notch signal transduction is compromised. Surprisingly, a recent study showed that a pancreas-specific compound knockout of *Notch1/2* had a very mild pancreatic phenotype without signs of deregulated *Neurog3* expression (Nakhai et al., 2008). However, this mild phenotype may be due to

[1]Department of Developmental Biology, Hagedorn Research Institute, Niels Steensens Vej 6, DK-2820 Gentofte, Denmark. [2]Department of Molecular Biology, University of Aarhus, DK-8000, Aarhus, Denmark. [3]Department of Molecular Biology, University of Texas Southwestern Medical Center, Dallas, TX 76390, USA. [4]Department of Cell and Developmental Biology, Vanderbilt University School of Medicine, Nashville, TN 37232-8240, USA.

*These authors contributed equally to this work
‡Author for correspondence (pas@hagedorn.dk)

**Accepted 28 October 2011**

timing of deletion, which was only shown to be efficient by E14.5, and/or due to possible compensatory activation of *Notch3/4* expression in the pancreatic epithelium, which was not excluded.

The function of *Hes1* downstream of Dll1-Notch-mediated lateral inhibition may not be the only function of Hes1 in pancreatic development. For example, *Hes1* mutants show ectopic pancreas formation (Fukuda et al., 2006; Sumazaki et al., 2004), but this has not been observed in other Notch pathway mutants. Furthermore, even though *Hes1* mRNA expression appeared downregulated in the dorsal pancreas endoderm in *Dll1* mutants at E9.5 (Apelqvist et al., 1999), not all cells lost Hes1 expression after Ptf1a$^{Cre}$-mediated deletion of *Rbpj* (Fujikura et al., 2007). It was proposed that the pancreatic buds contain different classes of progenitors with respect to their sensitivity to Rbpj-mediated Notch signaling and that other factors are involved in maintaining *Hes1* expression. Recently, Sox9 was shown to be required for expression of *Hes1* and normal proliferation of MPCs (Seymour et al., 2007), supporting the idea that *Hes1* expression may be controlled by multiple inputs.

Here we demonstrate that endodermal *Hes1* expression is independent of *Dll1* function between E8.0 and E9.0 and that onset of Ptf1a expression around E9.0 directly activates *Dll1* expression in MPCs. At this stage, *Hes1* expression in MPCs becomes *Dll1*-dependent. Accordingly, we demonstrate that the phenotypes of *Hes1*$^{-/-}$ and *Dll1*$^{-/-}$ embryos diverge at key points and that *Hes1/Dll1* double mutants display an intermediate phenotype. Moreover, we find that early pancreatic hypoplasia in *Dll1* mutants (Apelqvist et al., 1999) is independent of endocrine development and thus not caused by excessive endocrine differentiation and an associated depletion of progenitors. Instead, a reduced rate of proliferation in MPCs appears to be responsible. Unexpectedly, we find that *Hes1* is required to sustain normal Ptf1a protein expression for a brief period during bud formation. *Dll1* expression in turn also depends on *Hes1*, demonstrating that epistatically, *Hes1* acts both up- and downstream of *Dll1*. Collectively, our results suggest that Hes1 initially has Notch-independent effects, or alternatively that Dll1 and Hes1 are involved in spatiotemporally distinct activities of the Notch pathway. Additionally, our data demonstrate that Ptf1a via activation of *Dll1* stimulates MPC proliferation and contributes to *Hes1* activation, and thereby may indirectly contribute to maintaining high Ptf1a protein levels.

## MATERIALS AND METHODS

### Transgenic mouse lines

*Dll1*$^{tm1Gos}$ (*Dll1*$^{lacZ/+}$) (Hrabe de Angelis et al., 1997), *Tg*(*Hes1-EGFP*)$^{1Hri}$ BAC transgenic (Klinck et al., 2011), *Neurog3*$^{tTA/+}$ (Wang et al., 2009), *Ptf1a*$^{Cre/+}$ (Kawaguchi et al., 2002) and *Hes1*$^{+/-}$ (Ishibashi et al., 1995) mouse lines were all kept as heterozygotes and genotyped by PCR and Southern blotting as previously described. All animal experiments described herein were approved by the Institutional Animal Welfare Committee at Hagedorn Research Institute and by the Danish Authorities for Animal Research.

### Immunohistochemistry

Whole-mount immunofluorescent staining of embryos and dissected tissues was performed as previously described (Ahnfelt-Ronne et al., 2007b), except for the cleaved Notch1 staining, where the specimens were pretreated by heating in 10 mM sodium citrate, pH 6 in a boiling water bath for 1 hour. Primary antibodies: rat anti-E-cadherin (R&D Systems), 1:1000; rabbit anti-β-galactosidase (MP Biomedicals), 1:1600 or 1:5000 with Tyramide Signal Amplification (TSA) (PerkinElmer, USA); goat anti-Pdx1 (Beta Cell Biology Consortium), 1:10,000; rabbit anti-Neurog3 (Ahnfelt-Ronne et al., 2007b) 1:16,000 with TSA; mouse anti-Nkx6-1 (Pedersen et al., 2006), 1:1000; rabbit anti-Cleaved Notch1 (Cell Signaling), 1:100 with TSA; rabbit anti-GFP (Living Colors, Clontech), 1:2000 with TSA; goat anti-Sox17 (R&D Systems), 1:1000; guinea pig anti-glucagon (Millipore), 1:10,000; rabbit anti-Ptf1a (Hald et al., 2008), 1:20,000 with TSA; rabbit anti-Sox9 (Millipore), 1:500 with TSA. The samples were cleared in BABB (benzyl alcohol:benzyl benzoate1:2) before *z*-stack image scanning using a Zeiss LSM510 META Axio Imager connected to a LSM 510 laser module.

Immunofluorescent staining of 8 μm cryosections was performed as previously described (Hald et al., 2003). Primary antibodies: rabbit anti-β-galactosidase (MP Biomedicals), 1:1600; mouse anti-Neurog3 (Zahn et al., 2004), 1:500; goat anti-Pdx1 (Beta Cell Biology Consortium), 1:15,000; goat anti-GFP (Abcam), 1:1000; rabbit anti-Ptf1a (Hald et al., 2008), 1:4000.

### Chip-Seq analysis

Chromatin immunoprecipitation sequencing (ChIP-Seq) was performed as described (Masui et al., 2010). Briefly, chromatin was purified from E15.5 pancreata obtained from timed pregnant C57 mice and subjected to ChIP using rabbit anti-Rbpj serum raised against the peptide: NSSQVPSNESNTNSE or affinity-purified rabbit anti-mouse Ptf1a (Rose et al., 2001). Amplified libraries were prepared from the immunoprecipitated DNAs and sequenced with an Illumina/Solexa Genome Analyzer. 24.84, 16.77 and 5.99 million aligned tags were obtained for Ptf1a and Rbpjl ChIPs and input chromatin DNA, respectively. Peaks indicative of factor binding were determined with CisGenome 8 using default settings and a cut-off false discovery rate of 10E-5.

### Neurog3$^{+}$ cell quantifications

E9.0-9.5 dorsal pancreas buds were *z*-stack image scanned with the Achroplan 20×/0.5 W Ph2, WD 7.9 mm objective and Neurog3 positive cells were counted manually on every sixth section for 2.6 μm samples.

### Pancreatic bud volume quantifications

Quantification of bud volume was based on Pdx1 immunoreactivity in whole-mount *z*-stacks and quantified using the Imaris X64 software version 7.1.1 (Bitplane AG, Zurich, Switzerland). Surface-rendering-area detail was set to 2 μm. Thresholding was set to absolute intensity and manually adjusted to cover the Pdx1-positive area of the proper pancreas buds (not including any duodenal or bile duct epithelium).

### BrdU labeling and quantification

BrdU in saline suspension was injected at 100 μg/g intraperitoneally 1.5 hours before sacrifice. E10.5 embryos were fixed overnight in 4% formalin pH 7.0 and sectioned transversely at 200 μm on the vibratome. The sections were treated for 2 hours in 2 M HCl and subsequently stained using the protocol for whole-mount samples (see above). Primary antibodies: goat anti-Pdx1 (Beta Cell Biology Consortium), 1:10,000; rat anti-BrdU (Abcam), 1:500. After clearing in BABB, sections with dorsal pancreas were *z*-stack image scanned with the Plan-Neofluar 25×/0.8, WD 0.21 mm objective and the number of Pdx1-positive and Pdx1-BrdU double-positive cells were counted manually on every fourth optical section, or the sections were *z*-stack image scanned with the Achroplan 20×/0.5 W Ph2, WD 7.9 mm objective and counted manually on every second optical section.

### Whole-mount X-gal staining

E14.5 dissected *Dll1*$^{lacZ/+}$ pancreas was fixed for 2.5 hours in 4% formalin pH 7.0 and stained as described (Lobe et al., 1999).

## RESULTS

### *Dll1*, NICD and *Hes1* expression in early endoderm

To test predictions of the classical lateral inhibition model we first used immunofluorescence (IF) to map the expression patterns of *Dll1*, NICD and *Hes1* expression, relying on the β-galactosidase (β-gal) and EGFP reporters in *Dll1*$^{tm1Gos/+}$ (*Dll1*$^{lacZ/+}$ hereafter) mice (Hrabe de Angelis et al., 1997) and *Tg*(*Hes1-EGFP*)$^{1Hri}$ BAC transgenic mice (Klinck et al., 2011), respectively. We found β-gal expression in presomitic mesoderm and nascent somites in E8.25 embryos (Fig. 1A) and in scattered cells of the dorsal pancreatic

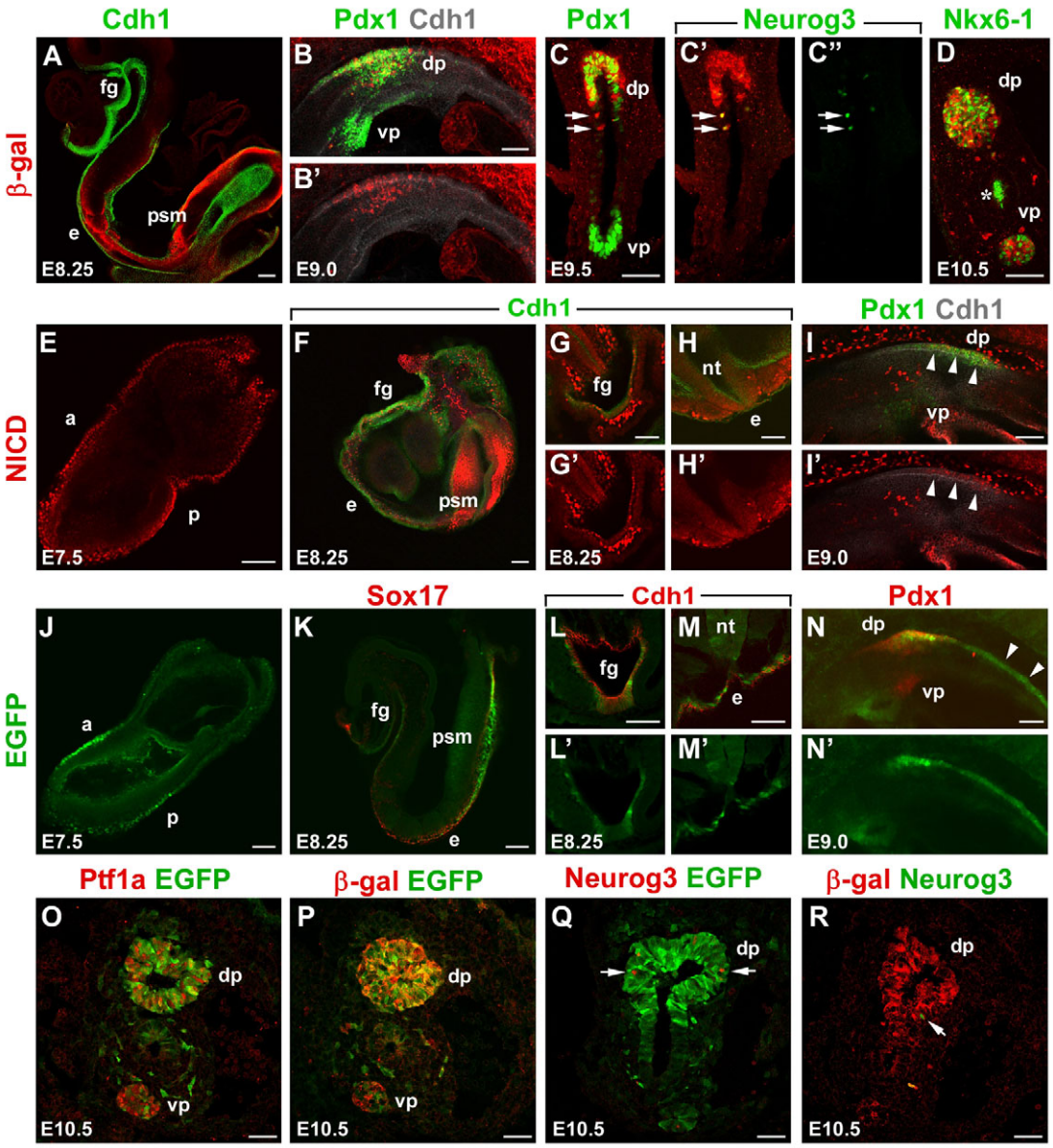


**Fig. 1. *Dll1*, NICD and *Hes1* expression in endoderm.** (**A-D**) Optical sections of E7.5 to E10.5 *Dll1*$^{lacZ/+}$ embryos whole-mount stained for β-galactosidase, Cdh1, Pdx1, Neurog3 or Nkx6-1. The arrows in C point to Neurog3$^{+}$ cells that co-express β-gal. The asterisk in D marks trapping of the anti-Nkx6-1 antiserum in the gut lumen. (**E-I'**) Optical sections of E7.5 to E9.0 wild-type embryos whole-mount stained for NICD and Cdh1. The arrowheads in I and I' indicate the NICD expression in the dorsal pancreatic epithelium. (**J-N'**) Optical sections of E7.5 to E9.0 *Tg*(*Hes1-EGFP*)$^{1Hri}$ embryos whole-mount stained for EGFP, Sox17, Cdh1 or Pdx1. The arrowheads in N point out Hes1-EGFP expression in the dorsal gut tube endoderm. (**O-R**) Cryosections of E10.5 *Dll1*$^{lacZ/+}$ *Tg*(*Hes1-EGFP*)$^{1Hri}$ double heterozygotes (O,P), *Tg*(*Hes1-EGFP*)$^{1Hri}$ (Q) and *Dll1*$^{lacZ/+}$ (R) embryos. (O) Double IF detection of Ptf1a and EGFP. (P) Double IF detection of β-galactosidase and EGFP. (Q) double IF detection of Neurog3 and EGFP. (R) Double IF detection of β-galactosidase and Neurog3. The arrows in Q and R point to Neurog3$^{+}$ cells. a, anterior; dp, dorsal pancreas; e, endoderm; fg, foregut; nt, neural tube; p, posterior; psm, presomitic mesoderm; vp, ventral pancreas. Scale bars: 50 μm. See also supplementary material Fig. S1.

endoderm of E9.0 *Dll1*$^{lacZ/+}$ embryos, whereas the ventral bud was negative (Fig. 1B). At E9.5, β-gal was expressed in Neurog3$^{+}$ cells and uniformly in the dorsal bud epithelium but absent from the ventral bud as well as the surrounding duodenal endoderm (Fig. 1C), consistent with previous analyses of *Dll1* expression by in situ hybridization (Apelqvist et al., 1999; Bettenhausen et al., 1995). Notably, a few Neurog3$^{+}$ cells were found in the lateral walls between the two pancreatic buds. Based on the timing of appearance, we speculate that these cells will join the dorsal glucagon cell cluster once differentiated. Alternatively, they may be the early precursors of enteroendocrine cells. At E10.5, β-gal expression was also found throughout the ventral bud epithelium (Fig. 1D) as well as in glucagon$^{+}$ cells of the dorsal bud, possibly due the long half-life of β-gal (not shown). β-gal expression was also seen in some endocrine precursors and in the developing acini at the secondary transition (supplementary material Fig. S1A-D). Consistent with previous work we did not detect expression of Jag1 in E10.5 pancreas (supplementary material Fig. S1E-G).

NICD immunoreactivity was seen in definitive endoderm already at E7.5 (Fig. 1E), coinciding with onset of *Hes1* expression (Fig. 1J). At E8.25, NICD and *Hes1* were broadly expressed in anterior and posterior endoderm, including the prospective pancreatic regions (Fig. 1F-H,K-M). From E9.0, NICD expression in the midgut region was confined to the dorsal pancreas bud (Fig. 1I, arrowheads) whereas *Hes1* additionally was expressed in a stripe in the prospective dorsal midgut (Fig. 1N, arrowheads).

Double IF for Ptf1a and Hes1-EGFP on *Dll1*$^{lacZ/+}$; *Tg*(*Hes1-EGFP*)$^{1Hri}$ showed extensive overlap of expression (Fig. 1O), as did double IF for β-galactosidase and EGFP on an adjacent section (Fig. 1P), indicating that Ptf1a and Dll1 also display extensive overlap of expression. By contrast, most of the β-galactosidase$^{+}$ and EGFP$^{+}$ cells were negative for Neurog3 (Fig. 1Q,R), but the few Neurog3$^{+}$ cells also appear positive for β-galactosidase and *Hes1* at E10.5. However, the long half-lives of both of our reporters (EGFP and *lacZ*) make it difficult to firmly conclude true co-expression.

To determine if endodermal Notch activation and *Hes1* expression depends on Dll1 activity, we analyzed NICD expression in wild-type and *Dll1*$^{lacZ/lacZ}$ embryos and EGFP expression in crosses of *Tg*(*Hes1-EGFP*)$^{1Hri}$ and *Dll1*$^{lacZ/+}$ mice. NICD expression was reduced in E10.5 *Dll1*$^{lacZ/lacZ}$ embryos compared with controls (Fig. 2A,B), but appeared to recover, approaching wild-type levels at E11.5 (Fig. 1C,D). Hes1-EGFP expression was normal in E8.25 *Dll1*$^{lacZ/lacZ}$ embryos (Fig. 1E,I) but had partly disappeared from the dorsal pancreas endoderm at E9.5 (Fig. 1F,J) and was almost lost at E10.5 (Fig. 1G,K). Remarkably, and coinciding with the reappearance of NICD, Hes1-EGFP expression was restored in E11.5 *Dll1*$^{lacZ/lacZ}$ embryos (Fig. 1H,L).

## Ptf1a is required for *Dll1* expression in MPCs

Although expression of *Dll1* was observed in Neurog3$^{+}$ cells as expected, we also noted expression in the remainder of the early dorsal pancreatic epithelium (Fig. 1C,D,P). It thus seems unlikely that Neurog3 can account for all *Dll1* expression in the pancreatic anlage. To test this notion we crossed *Dll1*$^{lacZ/+}$ onto a *Neurog3*$^{tTA/tTA}$ (*Neurog3* null mutant) background and analyzed for β-gal expression. We found strong β-gal expression in E10.5 *Dll1*$^{lacZ/+}$*Neurog3*$^{tTA/tTA}$ MPCs (Fig. 3B,E), demonstrating that *Dll1* expression in early MPCs is independent of Neurog3.

As basic helix-loop-helix (bHLH) proteins regulate *Dll1* expression in other tissues (Ito et al., 2000; Ma et al., 1998; Nelson and Reh, 2008; Yoon and Wold, 2000), and as the onset of *Dll1* expression in MPCs, as determined above, coincides with the onset of expression of the bHLH protein Ptf1a (Hald et al., 2008), we next tested if Ptf1a was required for *Dll1* expression in MPCs by crossing *Dll1*$^{lacZ/+}$ onto a *Ptf1a*$^{Cre/Cre}$ (*Ptf1a* null mutant) background and analyzing β-gal expression. Remarkably, β-gal expression was lost from Pdx1-expressing E10.5

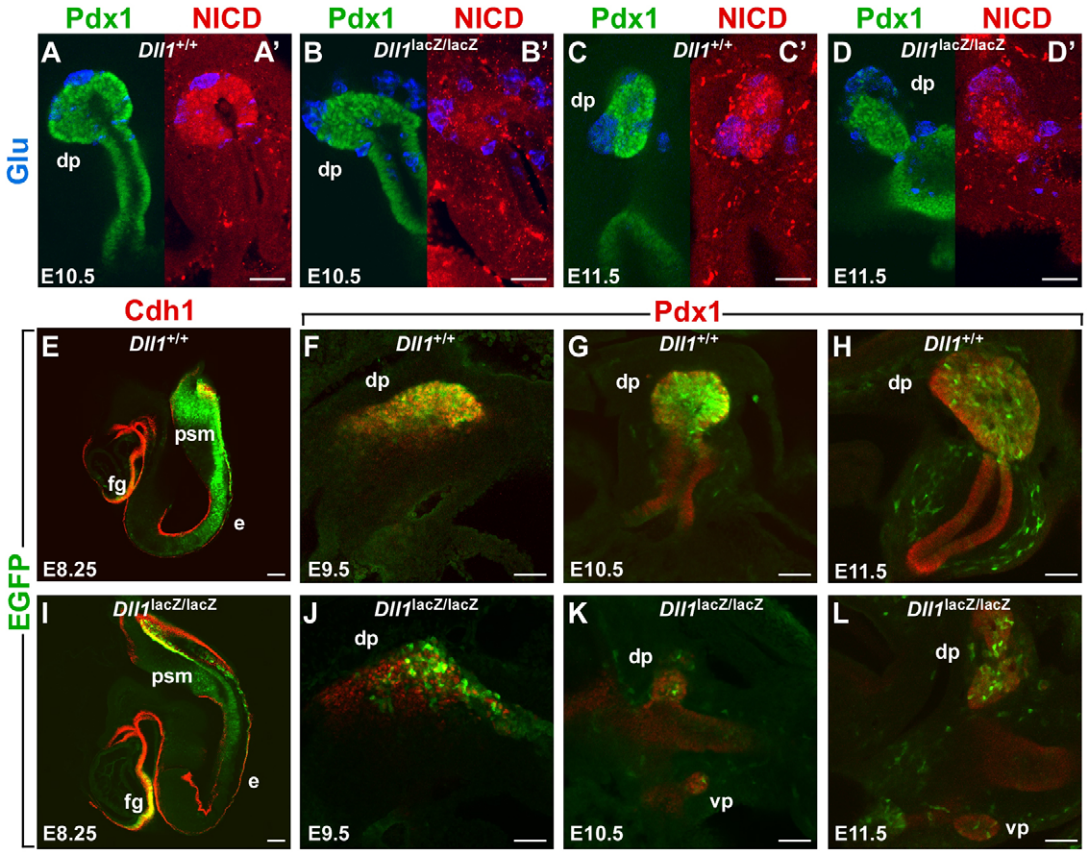


**Fig. 2. NICD and *Hes1* expression in *Dll1* mutants.** (**A-D**) Optical sections of whole-mount IF-stained E10.5 and E11.5 *Dll1*$^{+/+}$ and *Dll1*$^{lacZ/lacZ}$ embryos. The embryos were stained for Pdx1, NICD and glucagon. Note that NICD is reduced in E10.5 *Dll1*$^{lacZ/lacZ}$ embryos but recovers at E11.5. (**E-L**) Optical sections of *Tg*(*Hes1-EGFP*)$^{1Hri}$ mice on *Dll1*$^{+/+}$ (E-H) or *Dll1*$^{lacZ/lacZ}$ (I-L) background. Endodermal EGFP expression is normal in E8.25 *Dll1*$^{lacZ/lacZ}$ mice but becomes reduced beginning at E9.5 and is essentially lost at E10.5. However, EGFP expression recovers at E11.5 coincident with NICD recovery. dp, dorsal pancreas; e, endoderm; fg, foregut; psm, presomitic mesoderm; vp, ventral pancreas. Scale bars: 50 μm.

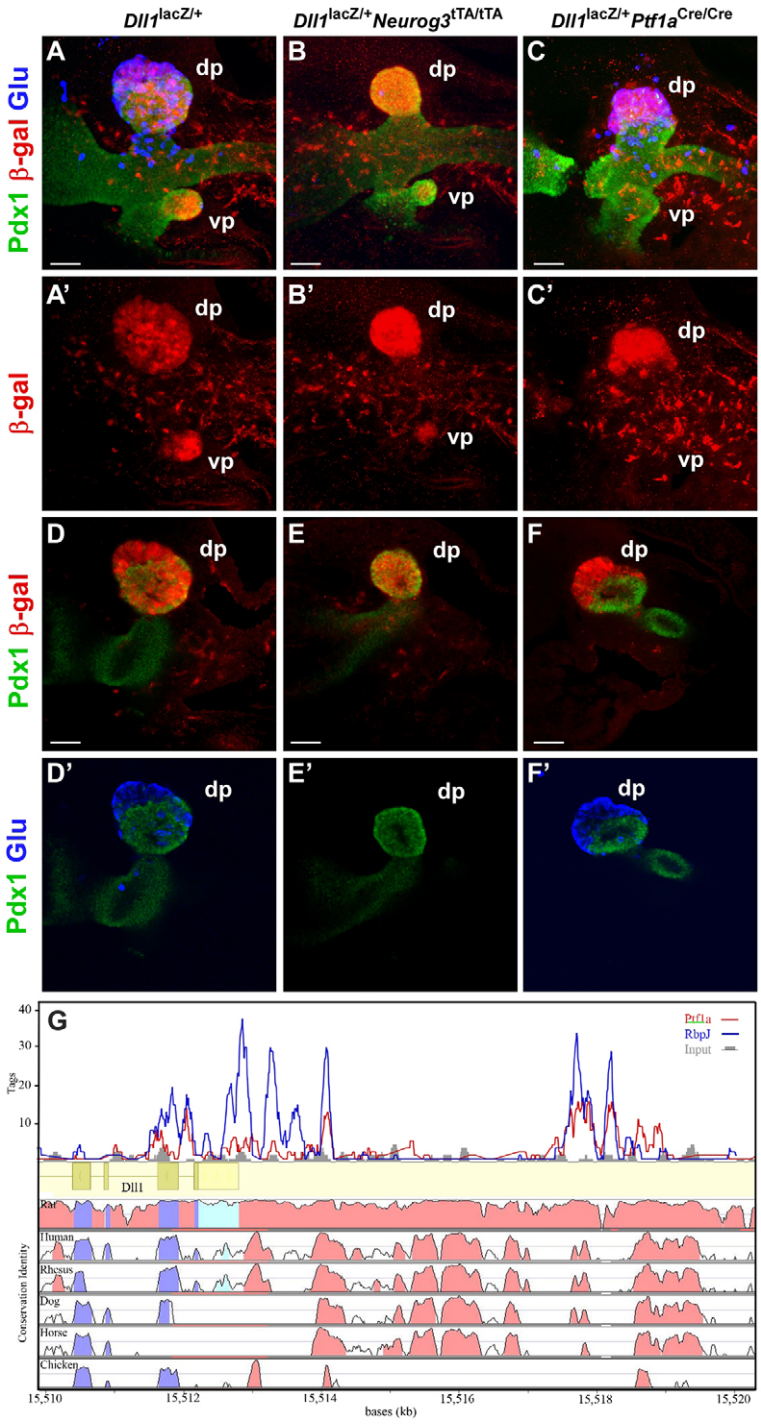


**Fig. 3. Ptf1a is required for Dll1 expression in MPCs.** (**A-F′**) Image stack projections (A-C) and optical sections (D-E) of whole-mount stained E10.5 embryos of the indicated genotypes, stained for β-galactosidase indicating *Dll1* expression, Pdx1 and glucagon. A-C show triple labeled projections. A′-C′ shows red channel alone for an unobstructed view of β-gal expression. D-F and D′-F′ show optical sections of red/green and blue/green channels, respectively, of the embryos shown in A-C. dp, dorsal pancreas; vp, ventral pancreas. Scale bars: 50 μm. (**G**) ChIP-Seq data obtained with anti-Ptf1a antibodies (red line) and anti-Rbpj antibodies (blue line) with E15.5 chromatin and aligned with a multiple sequence alignment of the *Dll1* 5′-flanking region. Note that Ptf1a and Rbpj bind to conserved sequences in the 5′-flank. Nucleotide positions on chromosome 17 are indicated. Note that the Dll1 locus depicted in G is on the lower strand and hence reads right to left. See also supplementary material Fig. S2.

*Dll1*$^{lacZ/+}$*Ptf1a*$^{Cre/Cre}$ pancreatic epithelial cells, but was retained in the endocrine lineage (Fig. 3C,F). It is possible that the loss of *Dll1* expression is a secondary effect of an overall cell fate change due to the absence of Ptf1a, but as Pdx1 is still expressed it is more likely that *Ptf1a* is required for *Dll1* expression in MPCs independently of *Neurog3* and the formation of endocrine progenitors in the early pancreas.

We then used ChIP-Seq analysis to test if Ptf1a could bind directly to regulatory sequences in the *Dll1* gene. As cell numbers are limited in E9.5 buds, we chose E15.5 pancreas where Ptf1a and Dll1 are co-expressed in developing acinar cells (not shown). As Ptf1a binds DNA together with Rbpj in early MPCs and Rbpjl in later acinar cells (Beres et al., 2006; Masui et al., 2007), we used antibodies against Ptf1a and Rbpj to perform the ChIP-Seq. We found that both proteins bound to the proximal promoter region of *Dll1* as well as to three or four sites in a conserved upstream region located from –4.7 to –6.4 kb upstream of the transcriptional start site (Fig. 3G). The peaks were discrete, present at other known Ptf1a-dependent regulatory sites (e.g. the Ptf1a enhancer, the Rbpjl promoter and Cpa1), statistically significant, and rare compared to the size of the genome (supplementary material Fig. S2A). Inspection of the nucleotide sequence revealed potential binding sites matching the consensus sequence (Beres et al., 2006) for the Ptf1a-Rbpj complex (supplementary material Fig. S2B). Although

these proposed binding sequences diverge somewhat from the consensus of either the E-box or the TC-box motifs (supplementary material Fig. S2B), this is not uncommon for bone fide binding sites of the Ptf1 complex (Beres et al., 2006; Masui et al., 2010). Together with the loss of *Dll1* expression in E10.5 Ptf1a mutant epithelium, these observations suggest that a Ptf1a-Rbpj complex might bind to *Dll1* regulatory sequences in early MPCs.

### *Dll1* is required for continued formation of endocrine precursors

The relevance of the classical lateral inhibition model was based on the previously reported similarity of *Dll1*, *Rbpj* and *Hes1* mutant phenotypes (Apelqvist et al., 1999; Jensen et al., 2000b) and the known role of homologs of these genes in *Drosophila* neuroblast specification where single cell suppression of neighbors via lateral inhibition is well documented (Simpson, 1990). However, the uncoupling of *Dll1* and *Hes1* expression and the *Neurog3* independent regulation of *Dll1* expression demonstrated above conflicts with predictions made by this canonical lateral inhibition model. Moreover, the different genetic backgrounds on which original analyses of *Dll1* and *Hes1* mutants were conducted might lead to differences in the extent and timing of precocious endocrine differentiation. This prompted us to reexamine the pancreatic phenotypes of *Dll1* and *Hes1* mutants on the same genetic background (CD1) and to examine *Dll1/Hes1* double mutants in order to determine the epistatic relationship between these two genes during early pancreas development.

We collected E8.5 to E12.5 wild-type and mutant embryos and analyzed the expression of Pdx1, Neurog3 and glucagon to view the pancreatic epithelium, endocrine precursors and differentiated endocrine cells, respectively, the latter predominantly expressing glucagon at these early stages (Jorgensen et al., 2007). To ensure sufficient sampling of all the tissue involved, we used whole-mount IF and high-resolution confocal microscopy (Ahnfelt-Ronne et al., 2007b) to obtain a global 3D view of the distribution of labeled cells. We found that *Hes1* (but not *Dll1*) mutants showed increased numbers of Neurog3$^+$ cells in dorsal endoderm as early as eight somites (~E8.25), just around the onset of dorsal Pdx1 expression and emergence of the earliest Neurog3$^+$ cells (Fig. 4A-C). At the 13-20 somite stage (~E9.0) we found a prominent increase in the number of Neurog3$^+$ cells in both *Dll1* and *Hes1* mutants as well as in *Dll1/Hes1* double mutants (Fig. 4E-H). However, while 21-28 somite (~E9.5) *Hes1* mutants still displayed increased numbers of Neurog3$^+$ cells compared with wild type, *Dll1* mutants showed a dramatic decrease in the number of Neurog3$^+$ cells (Fig. 4I-L), indicating that new Neurog3$^+$ cells were not formed given that Neurog3 is transiently expressed. This finding conflicts with that of Edlund and coworkers, who found increased numbers of Neurog3$^+$ cells at E9.5 (Apelqvist et al., 1999). We suspect that this conflict may be caused by the different genetic backgrounds that may cause a minor difference in the timing of precocious endocrine differentiation. Notably, *Dll1/Hes1* double mutants showed an intermediate phenotype with a mild excess of Neurog3$^+$ cells. Remarkably, the dorsal bud epithelium of double mutants appeared to show a depletion in Neurog3$^+$ cells, whereas excess Neurog3$^+$ cells were found in the lateral gut wall (Fig. 4L), a phenotype also seen in *Dll1* mutants heterozygous for *Hes1*, although the number of Neurog3$^+$ cells is smaller in these embryos (not shown). Quantification of Neurog3$^+$ cells confirmed that *Dll1*, *Hes1* and *Dll1/Hes1* mutant embryos had an equal increase of Neurog3$^+$ cells at the 13-20 somite stage and that *Dll1* mutants specifically showed a depletion of Neurog3$^+$ cells at the 21-28 somite stage (Fig. 4M). The mild excess of Neurog3$^+$ cells in double mutants is most likely the result of excess Neurog3$^+$ cells forming in the lateral gut wall combined with a depletion of Neurog3$^+$ cells in the dorsal bud itself.

Using the CD1 background, we could obtain living *Dll1* mutants until E12.5. At E11.0 the pancreatic epithelium was smaller than normal, as previously noted (Apelqvist et al., 1999). Neurog3$^+$ cells were far fewer, and this effect was maintained in E12.5 *Dll1* mutants (supplementary material Fig. S3). In contrast, *Hes1* mutants had numerous Neurog3$^+$ cells at these stages (supplementary material Fig. S3). Notably, from E10.5 onwards we found aberrant dorsal bud morphogenesis in *Hes1* mutants, a defect that may be associated with the ectopic pancreas found later in these animals (Fukuda et al., 2006; Sumazaki et al., 2004). We conclude that the Notch ligand Dll1 but not the Notch signaling effector Hes1 is required for the continued formation of Neurog3$^+$ endocrine precursors.

### Ptf1a-mediated *Dll1* expression is required for MPC proliferation

*Dll1* mutants have hypoplasia of the Pdx1$^+$ epithelium at E10.5, ostensibly caused by excessive differentiation and consequent depletion of Pdx1$^+$ progenitors (Apelqvist et al., 1999). However, the ventral bud is also reduced in size despite the absence of excessive endocrine differentiation (Fig. 5C), suggesting that another mechanism is responsible for the reduced size of the Pdx1$^+$ epithelium. If excessive endocrine development is causing the hypoplasia, then elimination of endocrine development should counteract it. To test this notion directly, we quantified dorsal and ventral bud sizes in E10.5 *Dll1*$^{lacZ/lacZ}$*Neurog3*$^{tTA/tTA}$ (double null) embryos, where endocrine development was expected to be abolished due to the absence of Neurog3 (Gradwohl et al., 2000). On a Neurog3 wild-type background, we found that dorsal and ventral bud volume was reduced ~5-fold in *Dll1*$^{lacZ/lacZ}$ mutants compared with controls (Fig. 5A,C,G). Remarkably, a similar fold reduction was observed in *Dll1*$^{lacZ/lacZ}$*Neurog3*$^{tTA/tTA}$ double null embryos, in spite of a drastic reduction of endocrine differentiation (Fig. 5F,G). Notably, *Neurog3*$^{tTA/tTA}$ embryos showed a modestly reduced dorsal bud size compared to wild types. The magnitude is, however, not sufficient to confound our conclusion about a role for Dll1 in epithelial growth independent of its inhibitory role in endocrine differentiation. Moreover, ventral bud size is not changed in *Neurog3*$^{tTA/tTA}$ embryos consistent with the very limited differentiation at this stage of ventral bud development. Nevertheless, ventral bud size is equally reduced in *Dll1*$^{lacZ/lacZ}$ and *Dll1*$^{lacZ/lacZ}$*Neurog3*$^{tTA/tTA}$ double null embryos (Fig. 5G), bolstering the notion of a Dll1 function independent of its inhibition of endocrine differentiation.

Surprisingly, a few endocrine cells were observed in the *Dll1* null and heterozygote background (*Dll1*$^{lacZ/lacZ}$*Neurog3*$^{tTA/tTA}$ and *Dll1*$^{lacZ/+}$*Neurog3*$^{tTA/tTA}$ embryos) compared with the complete loss of the endocrine lineage in *Dll1*$^{+/+}$*Neurog3*$^{tTA/tTA}$ embryos (Fig. 5D-F; data not shown). We speculate that this may be caused by derepression of other bHLH genes that could substitute for *Neurog3* and inefficiently initiate the endocrine commitment process on the *Dll1* mutant background. Nevertheless, the great reduction of endocrine differentiation should be sufficient to restore pancreatic epithelial development in *Dll1* mutants if depletion of progenitors was the cause of the hypoplasia. Notably, *Dll1*$^{lacZ/+}$ heterozygotes also showed reduced dorsal bud volume, on both wild-type and *Neurog3* deficient backgrounds (Fig. 5G), demonstrating *Dll1* haploinsufficiency.

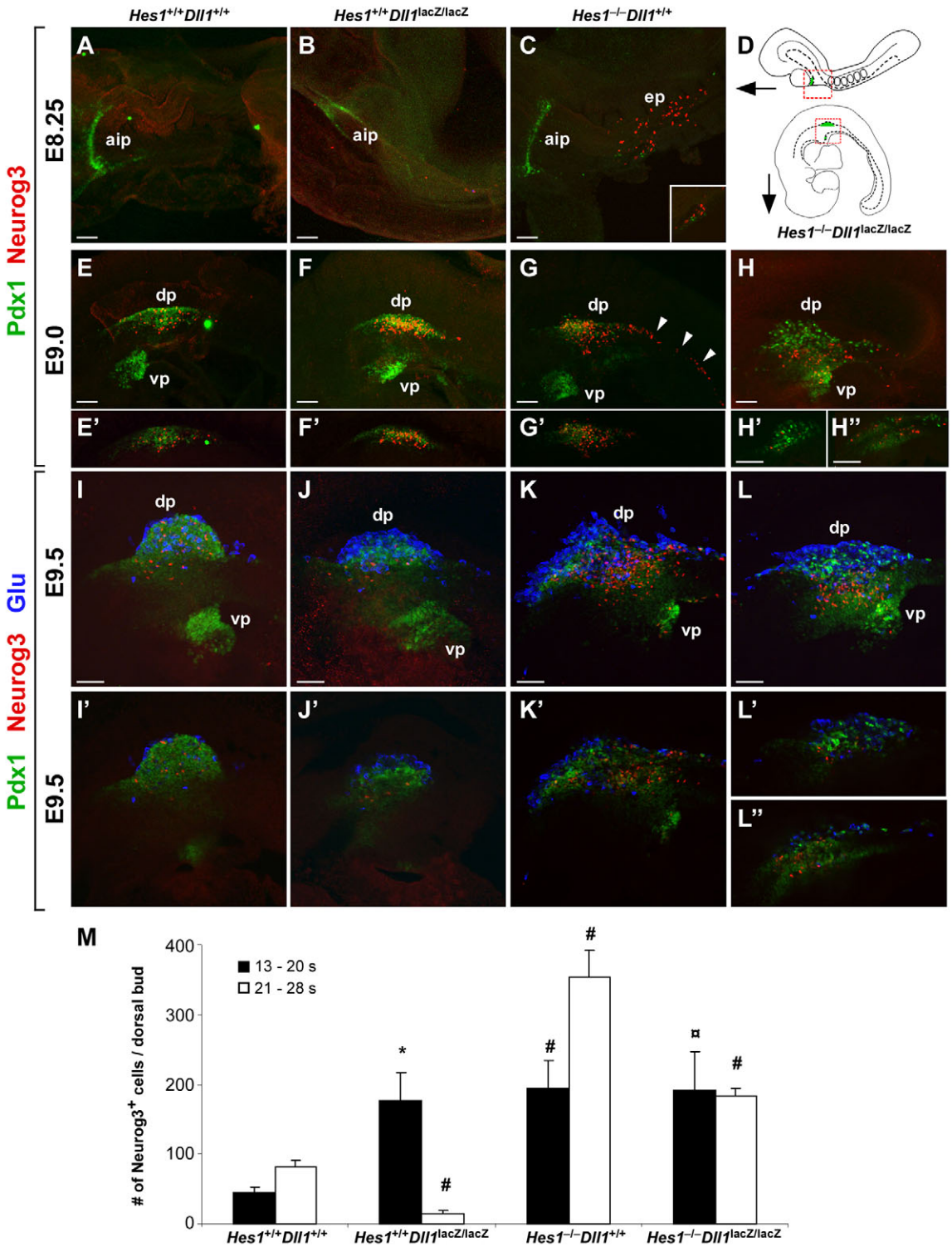


**Fig. 4. *Dll1* is required for continued formation of endocrine precursors.** (**A-C**) Image stack projections of E8.25 wild-type, *Dll1* and *Hes1* mutant embryos whole-mount stained for Pdx1 and Neurog3. The inset in C shows an optical section of emerging Pdx1$^+$ cells in the dorsal endoderm. Note that A and C are ventral views, whereas B is tilted more laterally. (**D**) Schematics of E8.25 and E9.0-9.5 embryos with red boxes indicating imaged areas in the other panels. (**E-H**) Image stack projections of E9.0 wild-type, *Dll1*, *Hes1* and *Hes1/Dll1* mutant embryos whole-mount stained for Pdx1 and Neurog3. The arrowheads in G point to ectopic expression of Neurog3 in the dorsal gut epithelium posterior to the Pdx1$^+$ pancreas area. (**E′-H′**) Optical sections through the dorsal bud region of the embryos shown in E-H. (**H″**) optical section through the lateral gut wall. (**I-L**) Image stack projections of E9.5 wild-type, *Dll1*, *Hes1* and *Hes1/Dll1* mutant embryos whole-mount stained for Pdx1, Neurog3 and glucagon. (**I′-L′**) Optical sections through the dorsal bud region of the embryos shown in I-L. (**L″**) Optical section through the lateral gut wall. aip, anterior intestinal portal; ep, endocrine progenitors; dp, dorsal pancreas; vp, ventral pancreas. Scale bars: 50 μm. (**M**) Bar graph showing quantification of Neurog3$^+$ cells in E9.0 (13-20 somite) and E9.5 (21-28 somite) wild-type, *Dll1*, *Hes1* and *Hes1/Dll1* mutant embryos. Data are represented as mean ± s.d. #, $P$<0.001; *, $P$<0.002; ¤, $P$<0.005; by Student's $t$-test (compared with wild type); $n$=3-9. See also supplementary material Fig. S3.

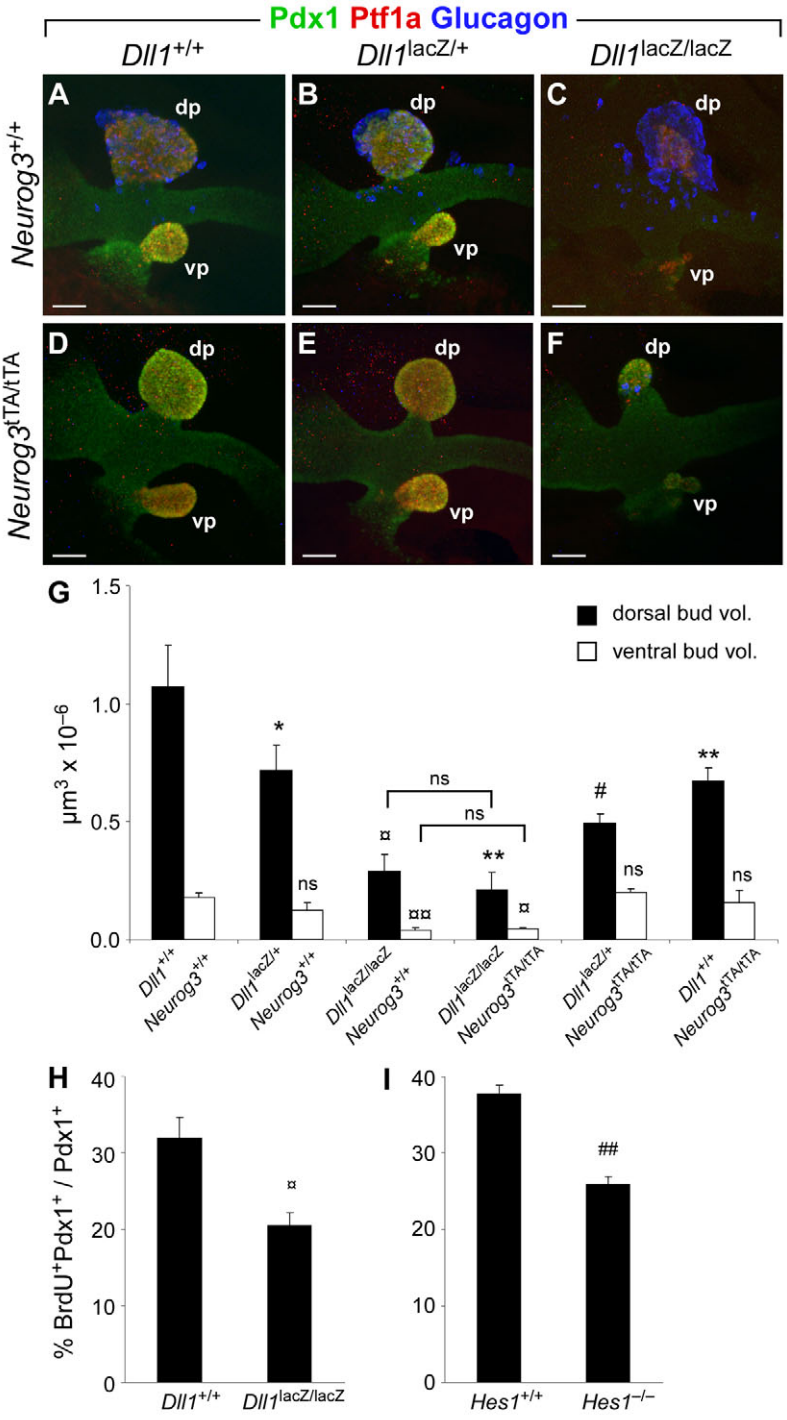


**Fig. 5. Ptf1a-mediated Dll1 expression is required for MPC proliferation.** (**A-F**) Image stack projections of E10.5 embryos from crosses of *Dll1*$^{lacZ/+}$*Neurog3*$^{tTA/+}$ double-heterozygote animals, whole-mount stained for Pdx1, Ptf1a and glucagon. Note that dorsal and ventral bud size is equally reduced in *Dll1*$^{lacZ/lacZ}$*Neurog3*$^{+/+}$ and *Dll1*$^{lacZ/lacZ}$*Neurog3*$^{tTA/tTA}$ embryos. dp, dorsal pancreas; vp, ventral pancreas. Scale bars: 50 μm. (**G**) Quantification of dorsal and ventral bud volume in wild-type and mutant embryos of the indicated genotypes based on Pdx1/Ptf1a double whole-mount stained and confocally scanned embryos. (**H**,**I**) Quantification of BrdU incorporation in E10.5 Pdx1$^{+}$ MPCs in *Dll1* and *Hes1* mutant dorsal buds, respectively. Data in G-I are represented as mean ± s.d. ##, $P<0.0002$; ¤¤, $P<0.0005$; #, $P<0.002$; ¤, $P<0.005$; **, $P<0.01$; *, $P<0.05$; by Student's *t*-test (compared with wild type unless otherwise indicated); $n$=2-4. ns, not significant.

Previous work ruled out apoptosis as a likely cause of pancreas hypoplasia in early *Dll1* mutants (Apelqvist et al., 1999), and forced activation of Notch signaling in pancreatic endoderm induces or maintains progenitor proliferation (Ahnfelt-Ronne et al., 2007a; Hald et al., 2003; Murtaugh et al., 2003). We therefore measured BrdU incorporation and found that it is reduced in *Dll1*$^{lacZ/lacZ}$ and *Hes1*$^{-/-}$ MPCs compared with wild-type controls (Fig. 5H,I), indicating that the hypoplasia seen in *Dll1* mutants is caused by reduced proliferation of MPCs. Moreover, the persistence of severe hypoplasia in *Dll1*$^{lacZ/lacZ}$*Neurog3*$^{tTA/tTA}$ double null embryos together with only moderate hypoplasia in *Neurog3* null embryos suggests that Ptf1a-induced *Dll1* expression is required for normal proliferation of MPCs.

## *Hes1* is required for normal Ptf1a expression in MPCs

A typical feature of the interactions between Notch signaling and the bHLH proteins that activate Notch ligand expression is a negative feedback loop in which activation of Notch signaling represses the expression and/or function of the cognate bHLH protein. Indeed, a previous report has shown that Hes1 can inhibit

the later 'acinar-differentiation-promoting' function of Ptf1a (Esni et al., 2004), and co-immunoprecipitation and yeast two-hybrid experiments have suggested that this inhibition might be mediated via a direct Hes1-Ptf1a protein-protein interaction (Ghosh and Leach, 2006). Nevertheless, Ptf1a activity is required in MPCs (Kawaguchi et al., 2002), and the concurrent expression with Hes1 seems to rule out that it inhibits all Ptf1a function at this earlier stage. In order to gain a better understanding of Hes1-Ptf1a interactions in early MPCs, we analyzed Ptf1a expression by whole-mount IF in E9.5 *Hes1*$^{-/-}$ embryos. Remarkably, we found that Ptf1a protein is lost from most of the dorsal (but not ventral), Pdx1$^{+}$ MPCs in *Hes1*$^{-/-}$ embryos compared with wild-type controls (Fig. 6A,B). By contrast, expression of Sox9, which is believed to act upstream of Hes1 (Seymour et al., 2007), was unaffected by the loss of Hes1 (Fig. 6C,D). The loss of Ptf1a protein in *Hes1*$^{-/-}$ embryos was also noticeable at E10.5 but had recovered by E12.5 (supplementary material Fig. S4).

The loss of Ptf1a protein in E9.5-10.5 *Hes1*$^{-/-}$ dorsal bud MPCs raises an intriguing possibility: as *Dll1* expression is dependent on Ptf1a at this stage (see above), one would predict that *Dll1* expression should be affected by the loss of Hes1, leading to an epistatic relationship between *Dll1* and *Hes1* that is in fact the opposite of that predicted by the classical lateral inhibition model. To test this notion, we compared *lacZ* expression in E9.5 and E10.5 *Dll1*$^{lacZ/+}$*Hes1*$^{-/-}$ and *Dll1*$^{lacZ/+}$*Hes1*$^{+/+}$ embryos. Remarkably, and as predicted by the loss of Ptf1a expression, β-gal expression was

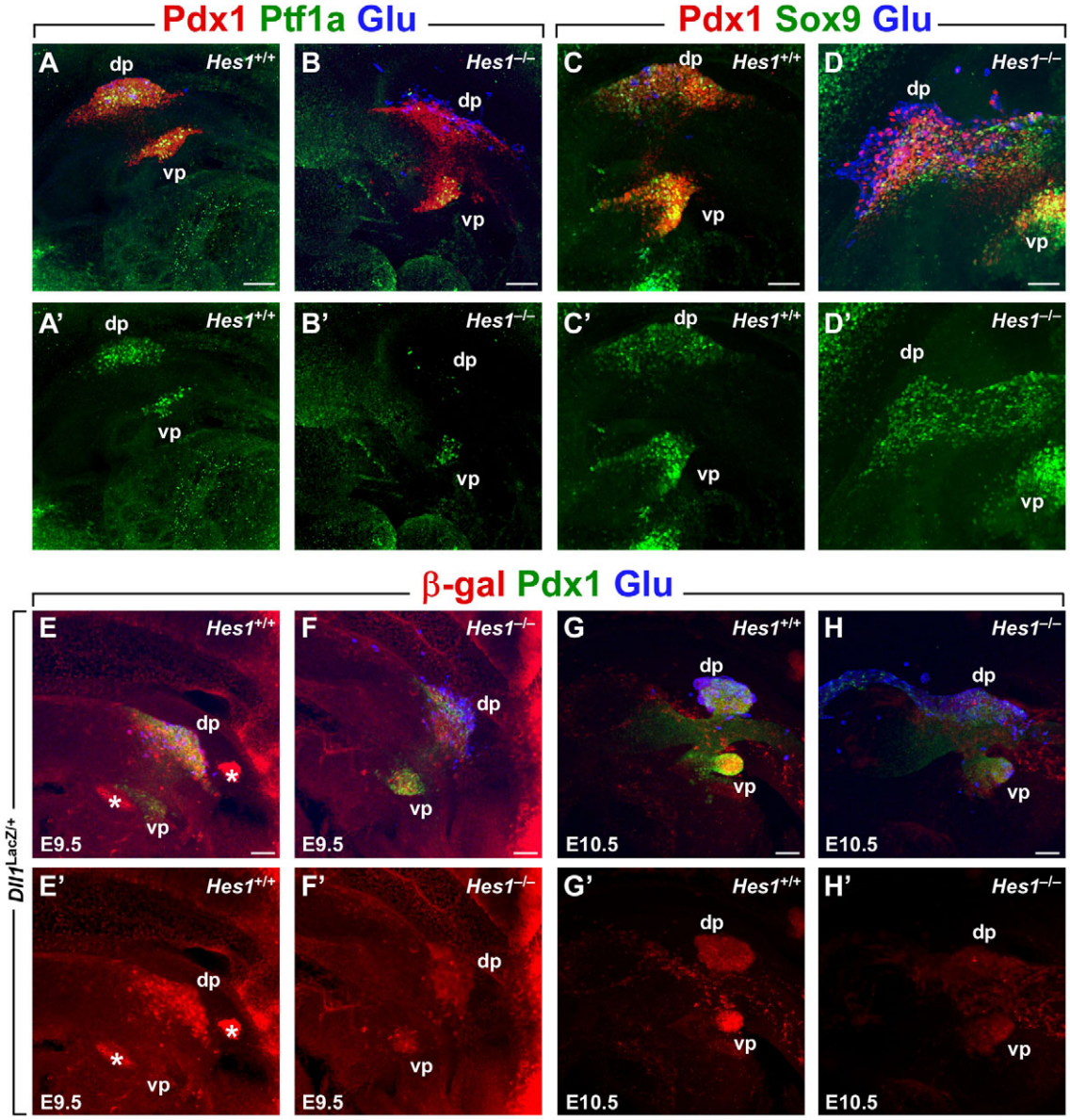


**Fig. 6. *Hes1* is required for normal Ptf1a and *Dll1* expression in MPCs.** (**A-D'**) Image stack projections of whole-mount stained E9.5 wild-type (A,C) and *Hes1*$^{-/-}$ (B,D) embryos, showing expression of Pdx1, glucagon and Ptf1a (A,B) or Sox9 (C,D). A'-D' show the green channel alone to give an unobstructed view. Note the loss of Ptf1a immunoreactivity in *Hes1*$^{-/-}$ dorsal bud. (**E-H'**) Image stack projections of whole-mount stained E9.5 (E,F) and E10.5 (G,H) wild-type (E,G) and *Hes1*$^{-/-}$ (F,H) embryos, showing expression of *Dll1* (β-gal), Pdx1 and glucagon. E'-H' show the red channel alone to give an unobstructed view. Note the reduced levels of β-gal expression in E9.5 and E10.5 dorsal buds and E10.5 ventral buds in *Hes1* mutants. The asterisks in E mark specks of non-specific fluorescence from the secondary antibody. dp, dorsal pancreas; vp, ventral pancreas. Scale bars: 50 μm. See also supplementary material Fig. S4.

reduced in E9.5 *Dll1*$^{lacZ/+}$*Hes1*$^{-/-}$ dorsal bud MPCs compared with *Dll1*$^{lacZ/+}$*Hes1*$^{+/+}$ controls (Fig. 6E,F). However, in the ventral bud, which normally does not express *Dll1-lacZ* at this stage (Fig. 1C and Fig. 5E), we observed the appearance of scattered β-gal$^{+}$ cells in *Dll1*$^{lacZ/+}$*Hes1*$^{-/-}$ embryos (Fig. 6F), presumably owing to the precocious appearance of *Dll1*-expressing, Neurog3$^{+}$ endocrine progenitors in the *Hes1* mutant background. Indeed, in addition to the loss of *Dll1-lacZ* from E10.5 dorsal buds, the normal onset of *Dll1-lacZ* expression in the ventral bud MPCs at this time is lost in *Dll1*$^{lacZ/+}$*Hes1*$^{-/-}$ embryos (Fig. 6G,H). Thus, Hes1 is required for normal levels of *Dll1* expression in MPCs.

## DISCUSSION

Based on the findings reported here, we propose that Ptf1a is a crucial transcriptional activator of *Dll1* expression, and therefore also of Notch signaling, in multipotent pancreatic progenitor cells. As a consequence of this mode of Notch activation, our results refute the classical lateral inhibition model proposed a decade ago (Apelqvist et al., 1999; Edlund, 2002; Jensen et al., 2000a; Skipper and Lewis, 2000). Our results also demonstrate a hitherto unsuspected requirement for *Hes1* in the maintenance of high Ptf1a protein levels and as a result also for normal *Dll1* expression. Thus, *Hes1* acts upstream of *Dll1* in addition to its role downstream of *Dll1*.

### Ptf1a-mediated activation of *Dll1* reveals a broader role for *Dll1* than classical lateral inhibition

We and others have previously provided evidence that Notch signaling, via its potential downstream target Hes1, regulates pancreatic endocrine development (Apelqvist et al., 1999; Jensen et al., 2000b). The classical lateral inhibition model puts forward that Neurog3-expressing endocrine progenitors signal to neighboring cells via Dll1 and instruct these to adopt alternate fates (e.g. pancreatic exocrine or persistence as MPCs). Lateral inhibition was proposed as the mechanism that coupled Notch signaling and *Hes1* expression to the regulation of *Neurog3* expression and endocrine differentiation. Nevertheless, more recent studies found no change in the number of Neurog3$^{+}$ cells in Ptf1a$^{Cre}$-mediated conditional Notch1/2-deficient embryos, while confirming that endocrine development was disturbed in conditional Rbpj knockouts (Nakhai et al., 2008). It was proposed that the requirement for Notch signaling in pancreatic development was less important than previously thought and that Rbpj may act independent of its role as a Notch effector. However, a requirement for Notch signaling during early pancreas development was not ruled out.

The results presented here demonstrate that Notch signaling is indeed essential during early, bud-forming stages of pancreatic development, from E8.0 to at least E10.5. Importantly, our observations on (1) the timing, extent and interdependency of *Dll1* and *Hes1* expression, (2) the Ptf1a-dependent expression of *Dll1* in MPCs, (3) the discordant phenotypes of *Dll1* and *Hes1* mutants, (4) the pancreatic hypoplasia of *Dll1*/*Neurog3* double null mutants and (5) the transient loss of Ptf1a protein and, in turn, *Dll1* expression in *Hes1*$^{-/-}$ MPCs, challenge the classical view of the lateral inhibition model. For example, *Hes1* is expressed in definitive endoderm (DE), long before *Dll1* becomes expressed in DE. Even so, the presence of NICD in E7.5 DE suggests that Notch signaling is active and that this may be responsible for activating Hes1 expression. Anteriorly, *Dll1* does not appear to be expressed at the right time and place to activate Notch in foregut DE, and we are not aware of other Notch ligands that are. Posteriorly, *Dll1* and *Dll3* is expressed in the adjacent presomitic mesoderm (Geffers et al., 2007), but it is not clear if Notch ligands expressed in presomitic mesoderm can signal across the basal lamina to activate Notch in DE. Nonetheless, Notch is activated and its target *Hes1* is expressed broadly in both anterior and posterior DE, but not via Neurog3-induced Dll1 expression. Indeed, *Dll1*-independent *Hes1* expression is evidenced by the continued expression of Hes1-GFP in *Dll1* mutant MPCs until E9.5. Later, at E10.5, both NICD and Hes1-GFP expression disappears from *Dll1* mutant dorsal bud epithelium, showing that *Hes1* expression becomes dependent on *Dll1* at this stage. The recovery of both NICD and Hes1-GFP expression in E11.5 *Dll1* mutants may be due to onset of *Jag1* expression around this time (Apelqvist et al., 1999) or due to the expression of non-canonical Notch ligands Dlk-1 (Carlsson et al., 1997) and/or Dner (J. Hald, personal communication) in the pancreatic epithelium around this time. While the lateral inhibition model correctly predicts Neurog3-dependent *Dll1* expression in endocrine progenitors, it fails to predict our observation of *Dll1* expression in MPCs as well as this expression being independent of Neurog3. The Ptf1a-dependent expression of *Dll1* in MPCs is likely to be through direct binding to conserved binding sites in the *Dll1* 5′-flanking region. Thus, Neurog3 and Ptf1a activate *Dll1* in endocrine progenitors and MPCs, respectively. A model incorporating the novel relationships between these transcription factors and Notch signaling components is presented in Fig. 7.

### *Dll1* is required for continued formation of endocrine progenitors

Refuting the classical lateral inhibition model prompted us to reexamine the pancreatic phenotypes resulting from deleting these genes, and to generate and examine *Dll1*/*Hes1* double mutants in order to elucidate the epistatic relationship between *Dll1* and *Hes1*. Overall, our results from these analyses are in agreement with previous studies but importantly, they reveal several features not previously appreciated that differ between the two mutants. First, the endocrinogenic phenotype of *Hes1* mutants is evident before the onset of *Dll1* expression in the pancreatic endoderm and before *Dll1* mutants show signs of endocrine development, supporting the idea that *Hes1* is acting independently of *Dll1* at this stage. Both single mutants and the double mutant show an equal increase in the number of Neurog3$^{+}$ cells at ~E9.0, which is similar in magnitude to that previously observed in the *Dll1* mutant by Apelqvist and coworkers (Apelqvist et al., 1999), but occurring half a day earlier than reported by this group. This difference in timing could be related to the different genetic backgrounds used.

From our 3D projections of whole embryos, it is evident that many of the Neurog3$^{+}$ cells found in *Hes1* mutants are located in the Pdx1$^{+}$ lateral gut walls between the dorsal and ventral pancreatic buds, while they are confined to the dorsal bud in *Dll1* mutants. Moreover, *Hes1* mutants show ectopic Neurog3$^{+}$ cells in the dorsal part of the prospective duodenum, exactly where we observe Hes1-GFP expression. Importantly, neither the lateral walls between the pancreatic buds nor the dorsal duodenum express *Dll1* (consistent with the lack of Ptf1a expression in these regions), showing that Hes1 can act independently of Dll1 not only dependent on the developmental stage but also depending on the exact location of the cells in the midgut region. The reduction of Neurog3$^{+}$ cells in E9.5 *Dll1* mutants stands in contrast to *Hes1* mutants, which maintain the increase seen at E9.0, and *Dll1*/*Hes1* double mutants, which show an intermediate phenotype with respect to Neurog3$^{+}$ cell numbers. Inspection of 3D projections

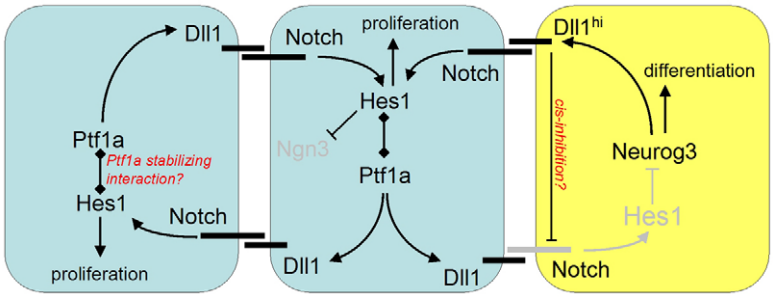


**Fig. 7. Model of the relationships between transcription factors and Notch signaling components in primary transition pancreas.** In contrast to the simple lateral inhibition model, the new model features Ptf1a-mediated activation of *Dll1*, which is crucial for Notch activation in MPCs. Furthermore, the model proposes that Notch is subject to cis-inhibition by high levels of Dll1 induced by Neurog3. Activated components of the regulatory system are shown in black, whereas components held inactive are gray.

revealed that the intermediate phenotype is related to the predominant location of endocrine precursors in the lateral gut walls in E9.5 *Dll1*/*Hes1* double mutants, with the dorsal bud being essentially devoid of Neurog3$^+$ cells as is also seen in E9.5 *Dll1* single mutants.

The loss of endocrine precursors in *Dll1* mutants has not previously been appreciated and is maintained until E12.5, the latest stage we could recover live embryos from. Loss of Neurog3$^+$ cells from E11.5, after an initial increase at E10.5, has been reported in conditional *Rbpj* mutants (Fujikura et al., 2006; Nakhai et al., 2008). However, it has been unclear if this is a consequence of compromised Notch signaling or the result of disrupting the function of the Ptf1a/Rbpj transcription factor complex (Fujikura et al., 2006; Nakhai et al., 2008). The similarity of *Dll1* and *Rbpj* mutant phenotypes in relation to Neurog3$^+$ cell numbers is consistent with the notion of loss of Neurog3$^+$ cells being due to loss of Notch signaling. Still, other explanations cannot be ruled out, and the cellular mechanism behind the depletion of Neurog3$^+$ cells remains unresolved. It has been proposed that an endocrine-restricted pool of progenitors adopt the endocrine fate prematurely when Notch signaling is compromised, resulting in depletion of this pool specifically while allowing continued development of exocrine progenitors (Fujikura et al., 2006; Nakhai et al., 2008). If this is the case, then Hes1 must act at least partly independent of Notch, as *Hes1* mutants have increased Neurog3$^+$ cells at least until E12.5.

An alternative explanation for the loss of endocrine precursors in *Dll1* mutants can be envisioned if one assumes that inhibitory Dll1-Notch interactions are required in cis for initiating and/or maintaining the endocrine differentiation program. Recent work has shown that cis-interactions between Notch and its ligands are crucial for preventing signal sending cells from receiving reciprocal signaling from their neighbors (Sprinzak et al., 2010). This notion offers an attractive mechanism for allowing formation of endocrine precursors during early pancreas development. We show here that *Dll1* expression in neighboring cells is under control of Ptf1a and not Neurog3. Thus, the regulatory logic from the classical lateral inhibition scheme, where high levels of Dll1 in the differentiating cell act via Notch to downregulate Neurog3 and in turn Dll1 in neighboring cells, breaks down. However, high levels of Neurog3-induced Dll1 might act in cis to prevent signaling to the differentiating cells from Ptf1a-induced Dll1 expression in neighboring MPCs, and thus allow differentiation to proceed in spite of continued Dll1 expression in adjacent MPCs. In such a model, endocrine precursors can form in *Dll1* mutants as long as no other Notch ligand is expressed in the MPCs (e.g. as seen in E9.0 *Dll1* mutants), but would be prevented when other Notch ligands become expressed in MPCs or if Notch becomes activated independent of canonical ligand expression. Further experiments determining (1) the onset of expression of other canonical and non-canonical Notch ligands and (2) whether conditional deletion of *Dll1* in endocrine precursors prevents their differentiation are needed to test this model.

## Ptf1a-mediated *Dll1* expression contributes to MPC proliferation and to maintaining Ptf1a protein levels

Ptf1a-induced *Dll1* expression in MPCs raises the question of whether this expression has a function besides preventing premature endocrine development. Previous work has suggested that Notch signaling stimulates MPC proliferation (Ahnfelt-Ronne et al., 2007a; Hald et al., 2003; Murtaugh et al., 2003), possibly via Hes1-mediated repression of *p57* expression (Georgia et al., 2006), and we show here that fewer *Dll1* (and *Hes1*) mutant MPCs incorporate BrdU than seen in wild-type controls, and that prevention of endocrine differentiation by eliminating *Neurog3* fails to restore the reduced bud size in *Dll1* mutants. Together these results suggest that the early pancreatic hypoplasia seen in *Dll1* mutants is caused by reduced proliferation of MPCs, rather than by depletion of MPCs by premature endocrine differentiation. It would thus seem that MPCs may exist in simultaneous sending and receiving states, contradicting the notion of these states being mutually exclusive (Sprinzak et al., 2010).

Ptf1a-dependent *Dll1* expression also raises the question about potential feedback regulation of Ptf1a itself. Loss of Ptf1a protein from most *Hes1*$^{-/-}$ dorsal bud MPCs, shows that *Ptf1a* transcription or Ptf1a protein expression depends on Hes1, at least briefly. Moreover, as we showed *Dll1* expression to be Ptf1a dependent, we could accurately predict that *Dll1* expression was reduced in *Hes1*$^{-/-}$ embryos. The mechanism behind this transient loss of Ptf1a remains obscure, but we speculate that potential protein-protein interactions between Ptf1a and Hes1 (Ghosh and Leach, 2006) may be involved. It is possible that Ptf1a and Hes1 are both part of a larger protein complex and that disruption of this complex in *Hes1* mutants destabilizes Ptf1a. Surprisingly, this places *Dll1* downstream of *Hes1* in addition to its role upstream of *Hes1* and suggests that Ptf1a, via Dll1, is contributing to *Hes1* activation and thereby may indirectly contribute to maintaining high Ptf1a protein levels.

In the present work we have exclusively analyzed early pancreatic development. Recent findings suggest even further complexity in Notch-mediated regulation of later pancreatic endocrine development (Cras-Meneur et al., 2009; Golson et al., 2009). Regardless of these later complexities in Notch-mediated regulation of pancreatic development, our results demonstrate that early pancreas development relies on Dll1-mediated Notch signaling to maintain normal proliferation of MPCs and to restrict early endocrine development by a mechanism that differs from the classical lateral inhibition model. These findings may have direct relevance for Notch-mediated control of endocrine differentiation in other parts of the gastrointestinal tract.

**Acknowledgements**
We are grateful to Ryochiro Kageyama for the *Hes1* mutants and to Mark Magnuson for help with generating *Neurog3* mutants. We thank Malene Jørgensen, Karsten Skole Markstrøm, and Søren Refsgaard Lindskog for expert technical assistance. We thank members of Department of Developmental Biology for constructive discussions.

**Funding**
This work was made possible by funding from the Danish Research Council for Health and Disease; the Juvenile Diabetes Research Foundation [1-2009-309]; the EU 6th Framework Program; and the National Institutes of Health [DK 072495 to P.S.]. Deposited in PMC for release after 12 months.

**Competing interests statement**
The authors declare no competing financial interests.

**Supplementary material**
Supplementary material available online at
http://dev.biologists.org/lookup/suppl/doi:10.1242/dev.071761/-/DC1

**References**

**Ahnfelt-Ronne, J., Hald, J., Bodker, A., Yassin, H., Serup, P. and Hecksher-Sorensen, J.** (2007a). Preservation of proliferating pancreatic progenitor cells by Delta-Notch signaling in the embryonic chicken pancreas. *BMC Dev. Biol.* **7**, 63.
**Ahnfelt-Ronne, J., Jorgensen, M. C., Hald, J., Madsen, O. D., Serup, P. and Hecksher-Sorensen, J.** (2007b). An improved method for three-dimensional reconstruction of protein expression patterns in intact mouse and chicken embryos and organs. *J. Histochem. Cytochem.* **55**, 925-930.
**Apelqvist, A., Li, H., Sommer, L., Beatus, P., Anderson, D. J., Honjo, T., Hrabe de Angelis, M., Lendahl, U. and Edlund, H.** (1999). Notch signalling controls pancreatic cell differentiation. *Nature* **400**, 877-881.
**Beres, T. M., Masui, T., Swift, G. H., Shi, L., Henke, R. M. and MacDonald, R. J.** (2006). PTF1 is an organ-specific and Notch-independent basic helix-loop-helix complex containing the mammalian Suppressor of Hairless (RBP-J) or its paralogue, RBP-L. *Mol. Cell. Biol.* **26**, 117-130.
**Bettenhausen, B., Hrabe de Angelis, M., Simon, D., Guenet, J. L. and Gossler, A.** (1995). Transient and restricted expression during mouse embryogenesis of Dll1, a murine gene closely related to Drosophila Delta. *Development* **121**, 2407-2418.
**Carlsson, C., Tornehave, D., Lindberg, K., Galante, P., Billestrup, N., Michelsen, B., Larsson, L. I. and Nielsen, J. H.** (1997). Growth hormone and prolactin stimulate the expression of rat preadipocyte factor-1/delta-like protein in pancreatic islets: molecular cloning and expression pattern during development and growth of the endocrine pancreas. *Endocrinology* **138**, 3940-3948.
**Cras-Meneur, C., Li, L., Kopan, R. and Permutt, M. A.** (2009). Presenilins, Notch dose control the fate of pancreatic endocrine progenitors during a narrow developmental window. *Genes Dev.* **23**, 2088-2101.
**Edlund, H.** (2002). Pancreatic organogenesis-developmental mechanisms and implications for therapy. *Nat. Rev. Genet.* **3**, 524-532.
**Esni, F., Ghosh, B., Biankin, A. V., Lin, J. W., Albert, M. A., Yu, X., MacDonald, R. J., Civin, C. I., Real, F. X., Pack, M. A. et al.** (2004). Notch inhibits Ptf1 function and acinar cell differentiation in developing mouse and zebrafish pancreas. *Development* **131**, 4213-4224.
**Fujikura, J., Hosoda, K., Iwakura, H., Tomita, T., Noguchi, M., Masuzaki, H., Tanigaki, K., Yabe, D., Honjo, T. and Nakao, K.** (2006). Notch/Rbp-j signaling prevents premature endocrine and ductal cell differentiation in the pancreas. *Cell Metab.* **3**, 59-65.
**Fujikura, J., Hosoda, K., Kawaguchi, Y., Noguchi, M., Iwakura, H., Odori, S., Mori, E., Tomita, T., Hirata, M., Ebihara, K. et al.** (2007). Rbp-j regulates expansion of pancreatic epithelial cells and their differentiation into exocrine cells during mouse development. *Dev. Dyn.* **236**, 2779-2791.
**Fukuda, A., Kawaguchi, Y., Furuyama, K., Kodama, S., Horiguchi, M., Kuhara, T., Koizumi, M., Boyer, D. F., Fujimoto, K., Doi, R. et al.** (2006). Ectopic pancreas formation in Hes1-knockout mice reveals plasticity of endodermal progenitors of the gut, bile duct, and pancreas. *J. Clin. Invest.* **116**, 1484-1493.
**Geffers, I., Serth, K., Chapman, G., Jaekel, R., Schuster-Gossler, K., Cordes, R., Sparrow, D. B., Kremmer, E., Dunwoodie, S. L., Klein, T. et al.** (2007). Divergent functions and distinct localization of the Notch ligands DLL1 and DLL3 in vivo. *J. Cell Biol.* **178**, 465-476.
**Georgia, S., Soliz, R., Li, M., Zhang, P. and Bhushan, A.** (2006). p57 and Hes1 coordinate cell cycle exit with self-renewal of pancreatic progenitors. *Dev. Biol.* **298**, 22-31.
**Ghosh, B. and Leach, S. D.** (2006). Interactions between hairy/enhancer of split-related proteins and the pancreatic transcription factor Ptf1-p48 modulate function of the PTF1 transcriptional complex. *Biochem. J.* **393**, 679-685.
**Golson, M. L., Le Lay, J., Gao, N., Bramswig, N., Loomes, K. M., Oakey, R., May, C. L., White, P. and Kaestner, K. H.** (2009). Jagged1 is a competitive inhibitor of Notch signaling in the embryonic pancreas. *Mech. Dev.* **126**, 687-699.
**Gradwohl, G., Dierich, A., LeMeur, M. and Guillemot, F.** (2000). neurogenin3 is required for the development of the four endocrine cell lineages of the pancreas. *Proc. Natl. Acad. Sci. USA* **97**, 1607-1611.
**Gu, G., Dubauskaite, J. and Melton, D. A.** (2002). Direct evidence for the pancreatic lineage: NGN3+ cells are islet progenitors and are distinct from duct progenitors. *Development* **129**, 2447-2457.
**Hald, J., Hjorth, J. P., German, M. S., Madsen, O. D., Serup, P. and Jensen, J.** (2003). Activated Notch1 prevents differentiation of pancreatic acinar cells and attenuate endocrine development. *Dev. Biol.* **260**, 426-437.
**Hald, J., Sprinkel, A. E., Ray, M., Serup, P., Wright, C. and Madsen, O. D.** (2008). Generation and characterization of Ptf1a antiserum and localization of Ptf1a in relation to Nkx6.1 and Pdx1 during the earliest stages of mouse pancreas development. *J. Histochem. Cytochem.* **56**, 587-595.
**Hrabe de Angelis, M., McIntyre, J., 2nd and Gossler, A.** (1997). Maintenance of somite borders in mice requires the Delta homologue Dll1. *Nature* **386**, 717-721.
**Ishibashi, M., Ang, S. L., Shiota, K., Nakanishi, S., Kageyama, R. and Guillemot, F.** (1995). Targeted disruption of mammalian hairy and Enhancer of split homolog-1 (HES-1) leads to up-regulation of neural helix-loop-helix factors, premature neurogenesis, and severe neural tube defects. *Genes Dev.* **9**, 3136-3148.
**Ito, T., Udaka, N., Yazawa, T., Okudela, K., Hayashi, H., Sudo, T., Guillemot, F., Kageyama, R. and Kitamura, H.** (2000). Basic helix-loop-helix transcription factors regulate the neuroendocrine differentiation of fetal mouse pulmonary epithelium. *Development* **127**, 3913-3921.
**Jensen, J., Heller, R. S., Funder-Nielsen, T., Pedersen, E. E., Lindsell, C., Weinmaster, G., Madsen, O. D. and Serup, P.** (2000a). Independent development of pancreatic alpha- and beta-cells from neurogenin3-expressing precursors: a role for the notch pathway in repression of premature differentiation. *Diabetes* **49**, 163-176.
**Jensen, J., Pedersen, E. E., Galante, P., Hald, J., Heller, R. S., Ishibashi, M., Kageyama, R., Guillemot, F., Serup, P. and Madsen, O. D.** (2000b). Control of endodermal endocrine development by Hes-1. *Nat. Genet.* **24**, 36-44.
**Jorgensen, M. C., Ahnfelt-Ronne, J., Hald, J., Madsen, O. D., Serup, P. and Hecksher-Sorensen, J.** (2007). An illustrated review of early pancreas development in the mouse. *Endocr. Rev.* **28**, 685-705.
**Kawaguchi, Y., Cooper, B., Gannon, M., Ray, M., MacDonald, R. J. and Wright, C. V.** (2002). The role of the transcriptional regulator Ptf1a in converting intestinal to pancreatic progenitors. *Nat. Genet.* **32**, 128-134.
**Klinck, R., Fuchtbauer, E. M., Ahnfelt-Ronne, J., Serup, P., Jensen, J. N. and Jorgensen, M. C.** (2011). A BAC transgenic Hes1-EGFP reporter reveals novel expression domains in mouse embryos. *Gene Expr. Patterns* **11**, 415-426.
**Kopinke, D., Brailsford, M., Shea, J. E., Leavitt, R., Scaife, C. L. and Murtaugh, L. C.** (2011). Lineage tracing reveals the dynamic contribution of Hes1+ cells to the developing and adult pancreas. *Development* **138**, 431-441.
**Lammert, E., Brown, J. and Melton, D. A.** (2000). Notch gene expression during pancreatic organogenesis. *Mech. Dev.* **94**, 199-203.
**Lobe, C. G., Koop, K. E., Kreppner, W., Lomeli, H., Gertsenstein, M. and Nagy, A.** (1999). Z/AP, a double reporter for cre-mediated recombination. *Dev. Biol.* **208**, 281-292.
**Ma, Q., Chen, Z., del Barco Barrantes, I., de la Pompa, J. L. and Anderson, D. J.** (1998). neurogenin1 is essential for the determination of neuronal precursors for proximal cranial sensory ganglia. *Neuron* **20**, 469-482.
**Masui, T., Long, Q., Beres, T. M., Magnuson, M. A. and MacDonald, R. J.** (2007). Early pancreatic development requires the vertebrate Suppressor of Hairless (RBPJ) in the PTF1 bHLH complex. *Genes Dev.* **21**, 2629-2643.
**Masui, T., Swift, G. H., Deering, T., Shen, C., Coats, W. S., Long, Q., Elsasser, H. P., Magnuson, M. A. and MacDonald, R. J.** (2010). Replacement of Rbpj with Rbpjl in the PTF1 complex controls the final maturation of pancreatic acinar cells. *Gastroenterology* **139**, 270-280.
**Murtaugh, L. C., Stanger, B. Z., Kwan, K. M. and Melton, D. A.** (2003). Notch signaling controls multiple steps of pancreatic differentiation. *Proc. Natl. Acad. Sci. USA* **100**, 14920-14925.
**Nakhai, H., Siveke, J. T., Klein, B., Mendoza-Torres, L., Mazur, P. K., Algul, H., Radtke, F., Strobl, L., Zimber-Strobl, U. and Schmid, R. M.** (2008). Conditional ablation of Notch signaling in pancreatic development. *Development* **135**, 2757-2765.
**Nelson, B. R. and Reh, T. A.** (2008). Relationship between Delta-like and proneural bHLH genes during chick retinal development. *Dev. Dyn.* **237**, 1565-1580.
**Pedersen, I. L., Klinck, R., Hecksher-Sorensen, J., Zahn, S., Madsen, O. D., Serup, P. and Jorgensen, M. C.** (2006). Generation and characterization of monoclonal antibodies against the transcription factor Nkx6.1. *J. Histochem. Cytochem.* **54**, 567-574.
**Rose, S. D., Swift, G. H., Peyton, M. J., Hammer, R. E. and MacDonald, R. J.** (2001). The role of PTF1-P48 in pancreatic acinar gene expression. *J. Biol. Chem.* **276**, 44018-44026.

**Schaffer, A. E., Freude, K. K., Nelson, S. B. and Sander, M.** (2010). Nkx6 transcription factors and Ptf1a function as antagonistic lineage determinants in multipotent pancreatic progenitors. *Dev. Cell* **18**, 1022-1029.
**Schwitzgebel, V. M., Scheel, D. W., Conners, J. R., Kalamaras, J., Lee, J. E., Anderson, D. J., Sussel, L., Johnson, J. D. and German, M. S.** (2000). Expression of neurogenin3 reveals an islet cell precursor population in the pancreas. *Development* **127**, 3533-3542.
**Seymour, P. A., Freude, K. K., Tran, M. N., Mayes, E. E., Jensen, J., Kist, R., Scherer, G. and Sander, M.** (2007). SOX9 is required for maintenance of the pancreatic progenitor cell pool. *Proc. Natl. Acad. Sci. USA* **104**, 1865-1870.
**Simpson, P.** (1990). Lateral inhibition and the development of the sensory bristles of the adult peripheral nervous system of Drosophila. *Development* **109**, 509-519.
**Skipper, M. and Lewis, J.** (2000). Getting to the guts of enteroendocrine differentiation. *Nat. Genet.* **24**, 3-4.
**Sprinzak, D., Lakhanpal, A., Lebon, L., Santat, L. A., Fontes, M. E., Anderson, G. A., Garcia-Ojalvo, J. and Elowitz, M. B.** (2010). Cis-interactions between Notch and Delta generate mutually exclusive signalling states. *Nature* **465**, 86-90.
**Sumazaki, R., Shiojiri, N., Isoyama, S., Masu, M., Keino-Masu, K., Osawa, M., Nakauchi, H., Kageyama, R. and Matsui, A.** (2004). Conversion of biliary system to pancreatic tissue in Hes1-deficient mice. *Nat. Genet.* **36**, 83-87.
**Wang, S., Jensen, J. N., Seymour, P. A., Hsu, W., Dor, Y., Sander, M., Magnuson, M. A., Serup, P. and Gu, G.** (2009). Sustained Neurog3 expression in hormone-expressing islet cells is required for endocrine maturation and function. *Proc. Natl. Acad. Sci. USA* **106**, 9715-9720.
**Yoon, J. K. and Wold, B.** (2000). The bHLH regulator pMesogenin1 is required for maturation and segmentation of paraxial mesoderm. *Genes Dev.* **14**, 3204-3214.
**Zahn, S., Hecksher-Sorensen, J., Pedersen, I. L., Serup, P. and Madsen, O.** (2004). Generation of monoclonal antibodies against mouse neurogenin **3**, a new immunocytochemical tool to study the pancreatic endocrine progenitor cell. *Hybrid Hybridomics* **23**, 385-388.